13th International Conference on
Structural Health Monitoring of Intelligent Infrastructure
DOI: 10.3217/978-3-99161-057-1-109

Towards Accurate Road Health Monitoring: A Damage Detection System Using FBG Sensors

Ali Golmohammadi [1*, 0000-0002-8144-2198], Navid Hasheminejad [1, 0000-0002-0796-6321], Aliakbar Ghaderiaram [2, 0000-0003-1947-4487], Wim Van den bergh [1, 0000-0002-0897-1392], David Hernando [1, 0000-0001-8284-5792]

[1] SuPAR Research Group, Faculty of Applied Engineering, University of Antwerp, Antwerp, Belgium
[2] Materials & Environment, Faculty of Civil Engineering & Geosciences, Delft University of Technology, Delft, Netherlands

Email: seyedali.golmohammaditavalaei@uantwerpen.be, navid.hasheminejad@uantwerpen.be, A.Ghaderiaram@tudelft.nl, wim.vandenbergh@uantwerpen.be, david.hernando@uantwerpen.be

ABSTRACT: Advancements in road infrastructure health monitoring through sensor networks offer a transformative solution to the limitations of traditional inspection methods by enabling more accurate, real-time assessments of structural conditions. However, once appropriate sensors are selected and deployed, a key challenge remains: converting raw sensor data into meaningful health indicators (HIs) that effectively capture structural changes indicative of potential damage. A health indicator (HI) is a crucial metric derived from structural health monitoring (SHM) data, designed to reflect the current condition and damage state of a monitored structure. This study presents a machine learning-based approach leveraging principal component analysis (PCA) to develop a sensitive and damage-specific HI by extracting and ranking the most relevant current features. The proposed method is first validated through experimental fatigue testing using a four-point bending machine under random thermal conditions. To further evaluate its effectiveness and reliability in real-world applications, the approach is applied to field data collected from a network of fiber Bragg grating (FBG) sensors embedded in asphalt pavement. By analyzing strain measurements, the study demonstrates that the PCA-based HI successfully detects structural changes, providing a robust and data-driven solution for real-time infrastructure monitoring.

KEYWORDS: Health indicator, Structural health monitoring, FBG sensor networks, Principal component analysis, Fatigue damage detection.

1 INTRODUCTION

A significant amount of money is spent on maintaining infrastructure such as roads, bridges, and other critical structures. To reduce maintenance costs, various non-destructive testing (NDT) methods have been employed to enable predictive maintenance strategies. However, these methods have certain limitations. For instance, most NDT techniques operate offline, making continuous structural evaluation impossible [1].

To address this challenges, extensive research has been conducted to integrate advanced sensor technologies for continuous and real-time Structural Health Monitoring (SHM). Sensors such as accelerometers [2-4], piezoelectric sensors [5-7], and acoustic emission sensors [8-10] have been explored for their ability to collect SHM data continuously, providing valuable insights for early damage detection and improved maintenance planning.

Recently, optical sensors have emerged as a promising technology for infrastructure monitoring due to their unique advantages, such as immunity to electromagnetic interference, lightweight design, and, most importantly, the capability for distributed or quasi-distributed measurements. These features make optical sensors highly suitable for real-time structural health monitoring, enabling continuous and precise data collection over long distances. Additionally, their durability and resistance to harsh environmental conditions enhance their reliability for long-term deployment in critical infrastructure such as bridges, tunnels, and pipelines [11-17].

Although optical sensors offer these advantages, their application in large-span structures generates an enormous amount of data, requiring specialized strategies for processing, compression, and reduction. Efficient data management techniques are essential to handle this influx of information while preserving critical insights for future interpretation and analysis. Developing advanced algorithms and intelligent data filtering methods can help optimize storage and computational efficiency without compromising the accuracy and reliability of structural health monitoring [18].

Various techniques can be integrated to accomplish this objective, including data reduction methods [19-20] and multi-sensor data fusion [21-22] at different processing levels. A structured approach involves organizing these steps to derive a health indicator (HI) that enables straightforward monitoring of a system's health status. HI is regarded as the most informative feature in SHM data [23] that can be obtained using different frameworks including statistical, signal processing, and machine learning . In the literature, different criteria have been proposed to define an optimal HI. First viewpoint (1VP) suggests that an ideal HI should exhibit monotonicity, which represents a consistent increasing or decreasing trend over time, prognosability, which reflects the distribution of a variable's final values, and trendability, which measures the similarity between different variable trajectories [24].

Alternatively, second viewpoint (2VP) emphasizes that an optimal HI should possess detectability, referring to its sensitivity in identifying the presence of faults, particularly the smallest detectable fault signatures at a given false-positive rate. It should also ensure separability, which is its ability to effectively distinguish between faulty and healthy states. Additionally, trendability is crucial, as the degradation trend of

DOI: 10.3217/978-3-99161-057-1-109

the HI should maintain a positive correlation with operational time following an initial fault. However, identifying an optimal HI that satisfies all three properties is not a straightforward task. In practice, once an HI demonstrates both detectability and separability, it can already be considered optimal [25]. In this study, the second point of view is adopted as the criteria for defining an optimal HI. The first perspective requires extensive run-to-failure data, which is often challenging to obtain in real-world scenarios due to limited data availability. Ultimately, the developed HI can serve as an input for a prognosis model to estimate the remaining useful life (RUL), which will be explored in future studies.

2 OBJECTIVE AND OVERALL METHODOLOGY

The primary objective of this study is to propose a framework that integrates both data reduction and fusion techniques to construct health indicators that effectively represent the damage levels of infrastructures, such as roads, monitored using high-density FBG sensor networks. This method can be applied to individual FBG sensors or groups of sensors within a fiber, where data fusion can be performed at the data level.

In this approach (see Figure 1), following data acquisition via an embedded FBG sensor network and the management of large-scale collected data, a series of signal processing steps is applied to the raw data to prepare them for further analysis [26]. Subsequently, time-domain FBG signal features—including peak width, peak duration, and energy—are extracted from each segment of the pre-processed data.

After conducting long-term monitoring over a predefined period, these features are ranked based on their monotonicity metric to retain only the most significant ones. When new data arrive, the extracted features are normalized relative to the training dataset. Following normalization, a feature fusion technique based on principal component analysis (PCA) is implemented to project these features into a reduced-dimensional space. Since the first principal component captures the direction with the highest gradient in the feature space, it serves as a suitable indicator for representing the health status of the structure.

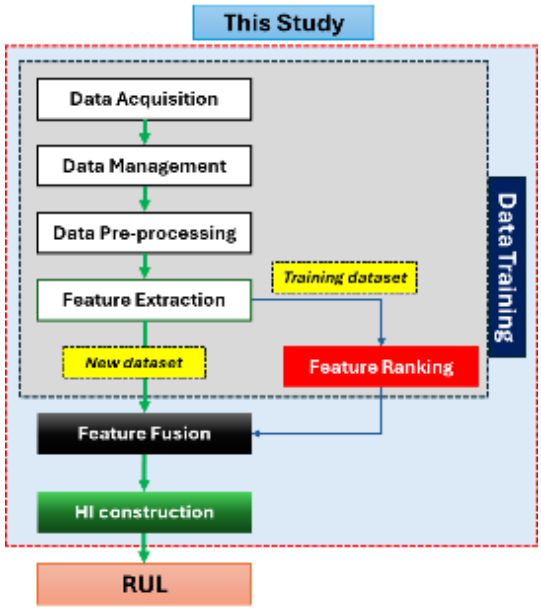

Figure 1. The overall framework of the study.

As no data is available on damage conditions from the embedded FBG sensor network, two approaches are used to evaluate the proposed framework. The first involves conducting an experimental fatigue test, while the second utilizes available FBG data to generate synthetic damage scenarios to validate its applicability. The following sections discuss these two approaches in detail.

3 METHODS

3.1 Data Acquisition

3.1.1 Experimental Fatigue Test

An experimental test was conducted to validate the proposed framework for large-scale, real-world damage detection applications. To achieve this, a stress-control fatigue experiment was performed using a four-point bending machine (see Figure 2) on a standard asphalt beam with dimensions of 60×60×400 mm, made from the APO-A mixture. The loading frequency was 10 Hz, and the temperature was varied randomly to simulate real-world conditions.

For the experiment, strain gauge (SG) sensors (3×10 and 3×20 mm) were installed to monitor strain at the bottom of the beam throughout the fatigue test, in order to further investigate the effect of strain gauge length on strain readings in asphalt materials. However, a detailed analysis of this effect is considered outside the scope of the present study. These SGs glued using CC-33A×5 adhesive, provided by KYOWA, between two internal supports. Strain data were collected using a compact recording system (EDX-10) at a sampling frequency of 500 Hz and subsequently processed using DCS-100A software.

Figure 2. Four-point bending setup for fatigue test.

After the test ended, the sample was damaged at the SG2 location, as shown in Figure 3a. The temperature recorded during the test is also presented in Figure 3b. Temperature data were collected using a thermocouple placed near the beam during testing.

DOI: 10.3217/978-3-99161-057-1-109

(a)

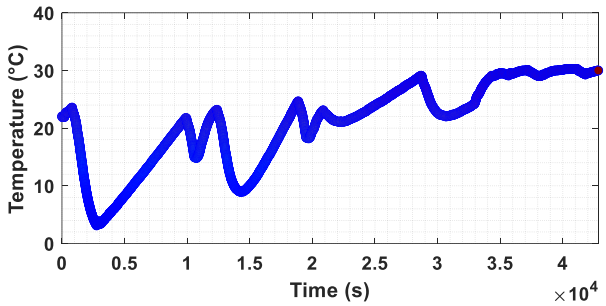

(b)

Figure 3. Fatigue test: (a) Damaged sample, (b) Temperature variations.

The strain data collected during the test using four strain gauges is presented in Figures 4a–4d.

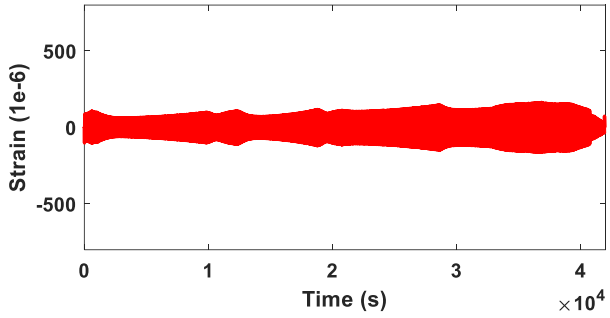

(a)

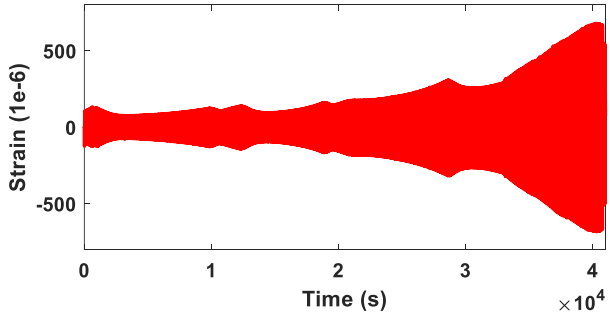

(b)

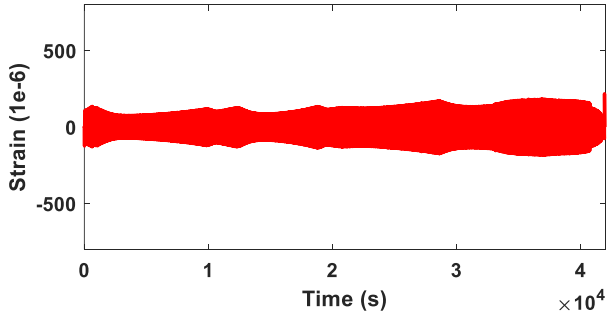

(c)

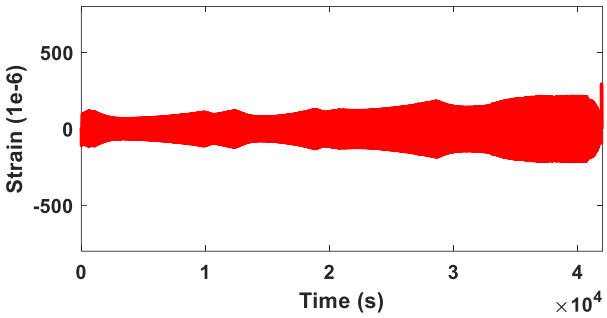

(d)

Figure 4. SG responses during fatigue test: (a) SG1, (b) SG2, (c) SG3, (d) SG4.

As shown in Figure 4, all SG responses exhibit load-induced strain signals after filtering out low-frequency components caused by temperature-induced strain. However, fluctuations in temperature can still influence the amplitude of the load-induced strain response due to temperature-dependent changes in material properties. As damage propagates, the responses of the strain gauges are affected depending on their location. If damage occurs at the sensor's location, an increasing trend will be observed due to strain concentration in that area. Conversely, if damage propagates near a sensor, its response will show a decreasing trend. However, this effect depends on the distance from the damaged region.

3.1.2 Field Test using FBG Sensor Network

In addition to the experimental fatigue test, strain and temperature data were collected using a FBG sensor network embedded in the asphalt layer at different locations on a constructed test track in the Port of Antwerp & Bruges. The sensor network configuration is shown in Figure 5, as can be seen this configuration includes 32 FBG in both lateral and longitudinal directions [27].

(a)

DOI: 10.3217/978-3-99161-057-1-109

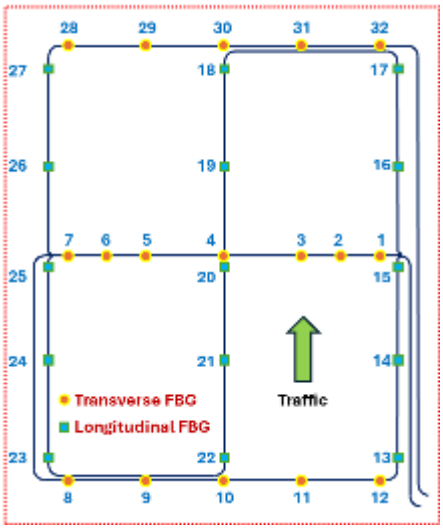

(b)

Figure 5. Monitoring system using FBG sensor network: (a) Test track, (b) FBG sensor configuration

After the construction of the test track, a continuous monitoring campaign was initiated from April 28, 2024, to October 17, 2024 (28/04/2024 to 17/10/2024), powered by a solar system and wind turbine. During this campaign, strain and temperature data were collected at a 100 Hz sampling frequency using an eight-channel, 2000 Hz FBG-Scan 708D interrogator. The collected data were then processed using ILLumiSense v2.3.5.5 software. Figure 6 shows the temperature variation in the asphalt during the monitoring campaign.

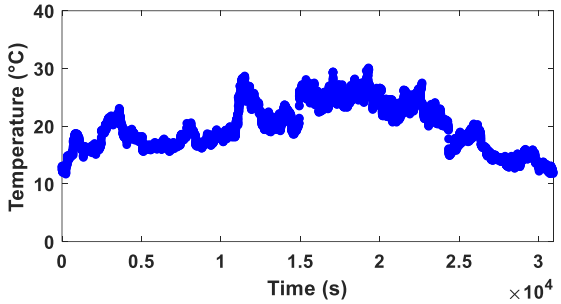

Figure 6 Temperature during the monitoring campaign collected by FBG sensor

3.2 *Data Management and Pre-processing*

During the monitoring campaign, 20 GB of data were generated daily, requiring efficient management to handle this large volume for future analysis. To address this, an automated system was developed to classify, merge, and prepare the data for subsequent steps, as outlined in Ref. [26].

Then, the data needs to be pre-processed using signal processing techniques to prepare it for the next steps. These steps include filtering, thresholding, concatenation, and windowing. Each technique is applied for a specific purpose: filtering removes strain caused by temperature variations, thresholding eliminates noise while preserving events, concatenation combines short-term monitored data into long-term datasets, and windowing ensures the data contains the same number of events for better comparison, as discussed in Ref. [26]. Figure 7 shows an example of the daily collected data alongside the long-term pre-processed FBG data.

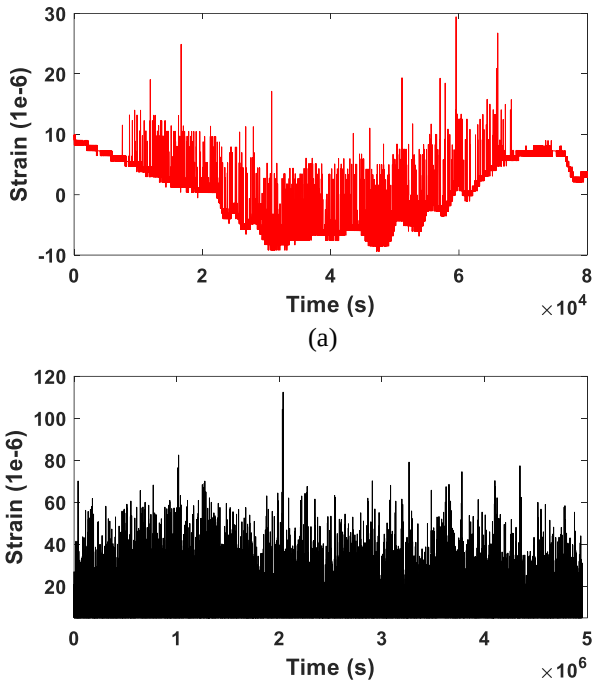

Figure 7 Collected FBG data during monitoring campaign: (a) daily data (17/05/2024), (b) long-term preprocessed data

3.3 *Feature Extraction*

Feature extraction plays a critical role in transforming raw data into meaningful, compact representations that can be efficiently used for analysis, classification, or prediction. As raw time-series or signal data is often too complex to interpret directly, extracting relevant features helps reduce dimensionality and focus on the most informative aspects of the data. This process not only improves model performance by providing more relevant input but also enhances the results, making it easier to identify underlying patterns or anomalies. In this study, several signal features in the time domain are calculated for each window of data [23], as listed in Table 1, along with peak width, peak duration, and energy. These features are essential for capturing the temporal characteristics of the signal and provide valuable insights into its behavior over time. Peak width and peak duration help describe the shape and spread of the signal's key events, while energy quantifies the overall magnitude of the signal, contributing to a more comprehensive understanding of its dynamics.

Table 1. Common statistical features in time-domain [23]

No	Equation	No	Equation
1	$X_m = \frac{\sum_{n=1}^{N} x(n)}{N}$	9	$X_{crest} = \frac{X_{peak}}{X_{rms}}$
2	$X_{sd} = \sqrt{\frac{\sum_{n=1}^{N}(x(n) - X_m)^2}{N-1}}$	10	$X_{clearance} = \frac{X_{peak}}{X_{root}}$
3	$X_{root} = \left(\frac{\sum_{n=1}^{N}\sqrt{\lvert x(n)\rvert}}{N}\right)^2$	11	$X_{shape} = \frac{X_{rms}}{\frac{1}{N}\sum_{n=1}^{N}\lvert x(n)\rvert}$
4	$X_{rms} = \left(\sqrt{\frac{\sum_{n=1}^{N}(x(n))^2}{N}}\right)$	12	$X_{impulse} = \frac{X_{peak}}{\frac{1}{N}\sum_{n=1}^{N}\lvert x(n)\rvert}$

DOI: 10.3217/978-3-99161-057-1-109

5	$X_{rss} = \left(\sqrt{\sum_{n=1}^{N} \lvert x(n)\rvert^2}\right)$	13	$X_{p2p} = \max(x(n)) - \min(x(n))$
6	$X_{peak} = max\lvert x(n)\rvert$	14-17	$X_{k\_cm} = \frac{\sum_{n=1}^{N}(x(n) - X_m)^k}{N}$
7	$X_{skewness} = \frac{\sum_{n=1}^{N}(x(n) - X_m)^3}{(N-1)X_{sd}^3}$	18	$X_{FM4} = \frac{X_{4\_cm}}{X_{st}^4}$
8	$X_{kurtosis} = \frac{\sum_{n=1}^{N}(x(n) - X_m)^4}{(N-1)X_{sd}^4}$	19	$X_{med} = \frac{\sum_{n=1}^{N} t(n)}{N}$

$x(n)$ indicates the signal sequence for $n = 1,2,\dots,N$.
N indicates the number of data points.
$t(n)$ indicates the moments of occurrence of $x(n)$

3.3.1 Feature Ranking

To determine the most relevant feature and develop an appropriate indicator, researchers have employed a specific metric in various studies [28]. This metric, known as monotonicity, captures the dominant increasing or decreasing trend of a feature concerning the target variable. It assesses how consistently a feature progresses in a specific direction. The monotonicity of the ith feature x_i is computed using the following equation:

$$Monotonocity\ (x_i) = \frac{1}{m}\sum_{j=1}^{m} \frac{\left|number\ of\ positive\ diff\left(x_i^j\right) - nummber\ of\ negetive\ diff(x_i^j)\right|}{n-1} \quad (1)$$

Where n represents the number of windows, and m denotes the number of monitored systems or structures, which, in our case, is 1. In this study, the metric is computed using the training datasets to identify the most important features for subsequent steps.

3.4 Feature Fusion

In this step, the most important selected features need to be fused to create a more informative and compact representation in lower dimensions while preserving as much relevant information as possible. Feature fusion helps reduce redundancy and enhances the efficiency of subsequent analyses. In this study, PCA is employed as a dimensionality reduction technique to fuse the selected features. PCA transforms the original feature set into a new set of uncorrelated principal components, ranked by their ability to capture variance in the data.

Before applying PCA, it is crucial to standardize the data to ensure that all features contribute equally to the analysis. Standardization prevents features with larger magnitudes from dominating the principal components. As a best practice, features should be normalized to the same scale before performing PCA. The mean and standard deviation used for normalization using z-score function, along with the PCA coefficients, are derived from the training data and consistently applied to the entire dataset.

4 IMPELLIMENTATION ON EXPERIMENTAL DATA

Four strain data sets are available from the SGs for the experimental test, based on the proposed methodology. As the data has already been managed and pre-processed using the DCS-100A software, the next step is feature extraction. In this step, the features mentioned in Section 3.3 are calculated for the SG signals by segmenting the signals into windows of 2,000 data points. Figure 8 presents examples of the features calculated for the SG signals.

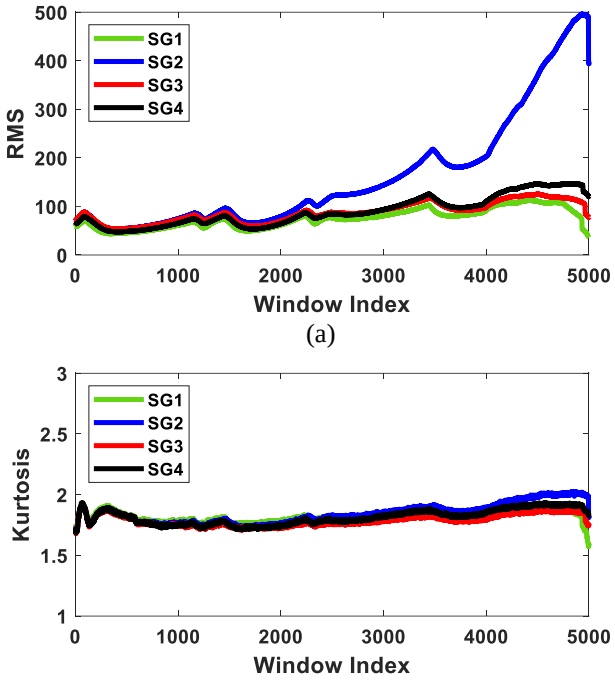

Figure 8 Examples of calculated features for SG sensors

After calculating these features, feature ranking is performed using Equation (1). However, the features are smoothed to enhance the performance of the monotonicity function. In this study, a threshold value of 0.3 is applied to select features for fusion. Figure 9 illustrates the feature importance for each SG. This feature ranking step is conducted using the training dataset, which represents 40% of the total lifetime.

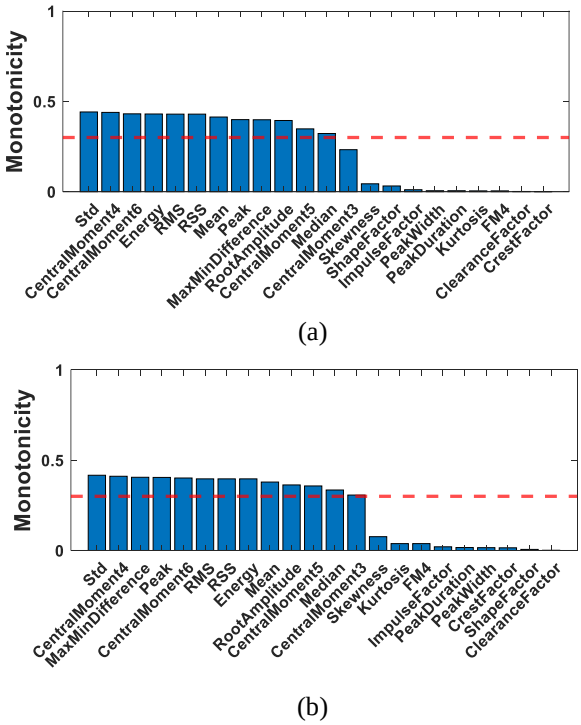

DOI: 10.3217/978-3-99161-057-1-109

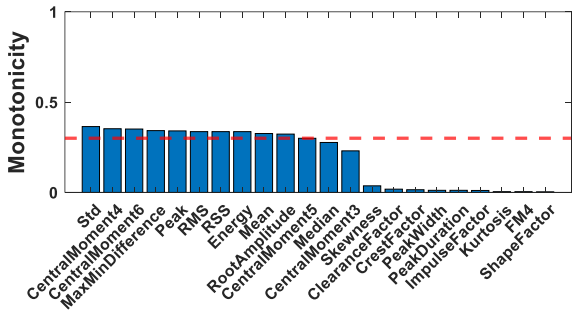

(c)

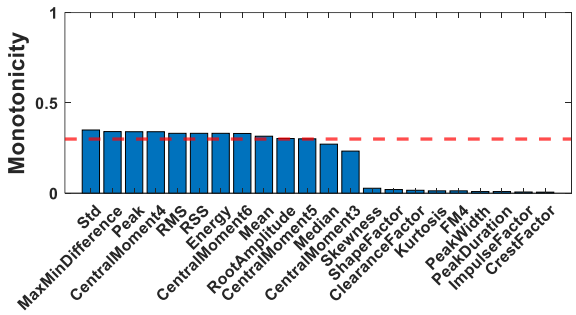

(d)

Figure 9 Feature importance: (a) SG1, (b) SG2, (c) SG3, (d) SG4

Based on Figure 9, it can be concluded which features exhibit greater importance and maintain a more monotonic trend during the fatigue test. For instance, the standard deviation demonstrates the highest importance across all SG sensors. Therefore, all selected features that meet the predefined threshold will be utilized for fusion.

For each SG sensor, the selected features are transformed to a lower-dimensional space using PCA, with normalization applied relative to the training dataset. The first principal component (PC) is chosen as it captures the maximum gradient in the feature space. Figure 10 illustrates the first principal component for each SG sensor based on the selected features.

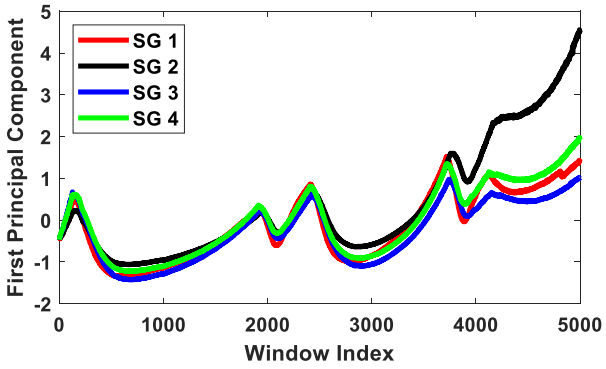

Figure 10 First principal component for each SG sensor

As shown in Figure 10, the first PC appears to be a promising HI derived from the fused features, offering greater robustness compared to any single feature. For better visualization of the first PC as a health indicator, an exponential function is fitted to each curve, with all curves shifted to zero at the starting point, as shown in Figure 11.

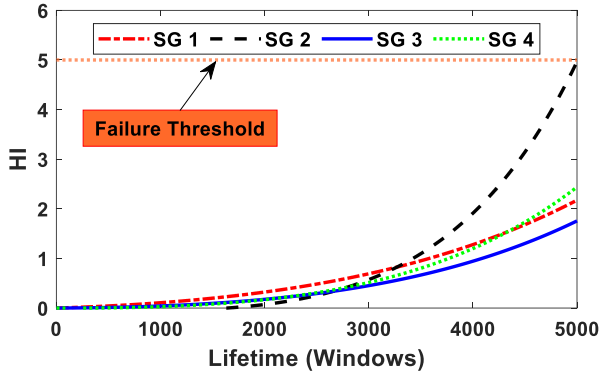

Figure 11 Constructed HI using SG sensor data

As shown in Figure 11, the HI for SG sensor 2 reaches level 5, which is recognized as the failure threshold. Therefore, this threshold can be used as a criterion for any new sample. However, due to the heterogeneous nature of asphalt, more experiments are required to establish a reliable threshold. Once validated, this HI can serve as an input to a prognosis model, such as an exponential degradation model, for estimating the remaining useful life. However, applying this approach in real field conditions remains challenging, as the exact failure point is still unknown.

5 IMPLEMENTATION ON IN-SITU DATA

Before implementing a method on in-situ data collected through an FBG sensor network embedded in the road, it is important to consider that, since the pavement sill is newly constructed, no damage is typically present, and the collected data can be labeled as "healthy." This dataset can then be used to generate synthetic data representing damaged conditions. Unlike experimental tests, where loading conditions are controlled, in this case, the loading is random, and no specific information about it is available. Based on experimental observations, damage affects sensor responses depending on its distance from the sensor. Therefore, two types of data can be generated: one where the damage occurs at the sensor location (G1) and another where the damage is not at the sensor location but within a detectable distance (G2). This can be achieved using an exponential function to generate synthetic data, as illustrated in Figure 12.

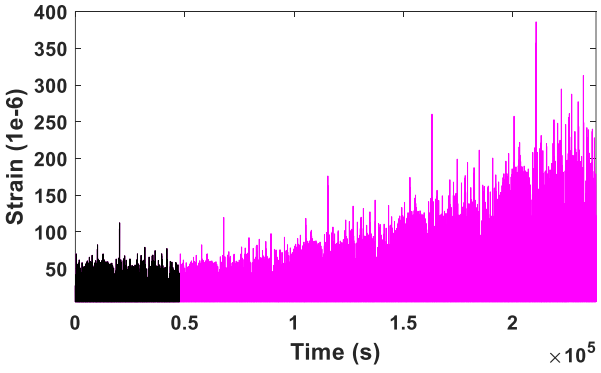

(a)

DOI: 10.3217/978-3-99161-057-1-109

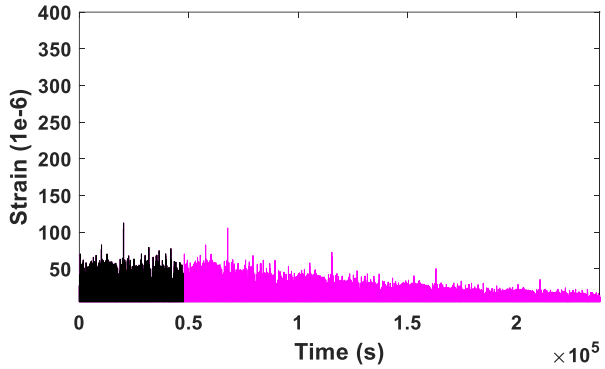

(b)

Figure 12 Generated synthetic data using available healthy data: (a) G1, (b) G2

Now, these data can be used to implement the proposed method, beginning with feature extraction. For example, Figure 13 shows the calculated features for both signals after segmentation into windows of 2,000 data points.

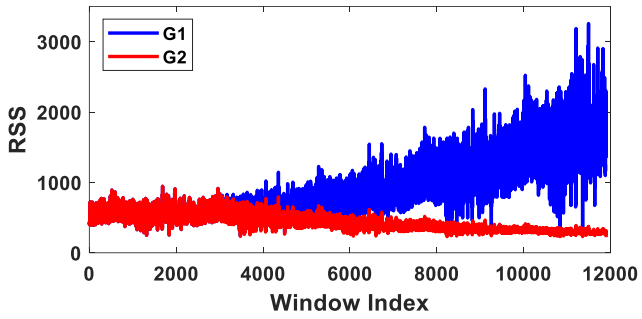

(a)

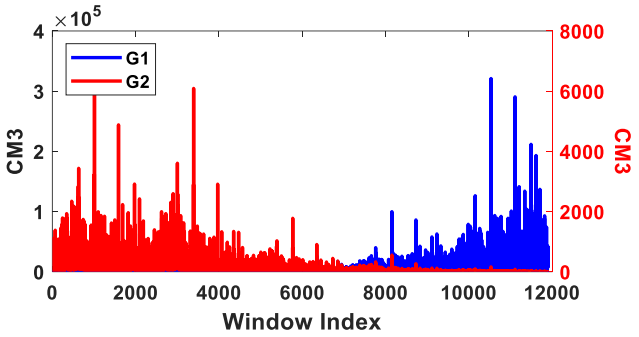

(b)

Figure 13 Examples of calculated features for G1 and G2

A threshold value of 0.3 is applied again to select features for fusion. Figure 14 illustrates the feature importance for G1 and G2. This feature ranking step is performed using the training dataset, which accounts for 40% of the total lifetime.

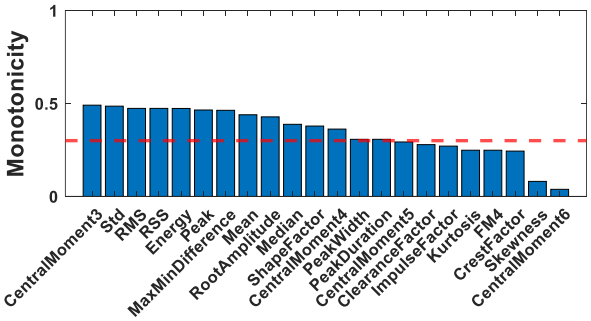

(a)

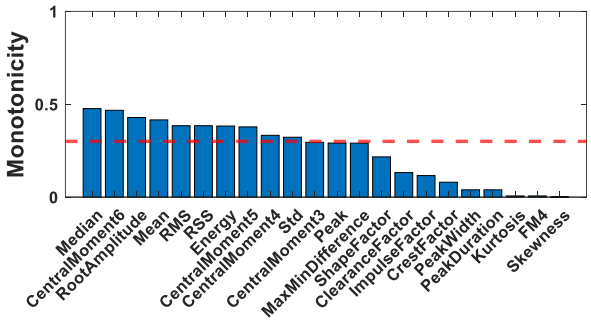

(b)

Figure 14 Feature importance: (a) G1, (b) G2

As shown in Figure 14, the important features vary in each case. For example, in the first case, central moment 3 is the top feature, whereas in the second case, it is not even among the selected features. This highlights the importance of feature ranking before fusion. Figure 15 illustrates the first principal component for each generated data based on the selected features.

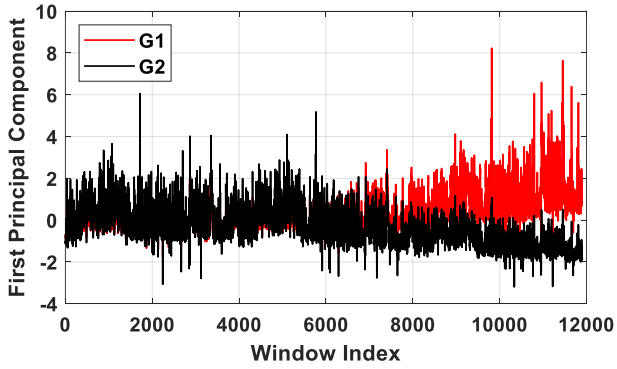

Figure 15 Feature importance: (a) G1, (b) G2

For clearer visualization of the PC as a health indicator, an exponential function is fitted to each curve, with all curves adjusted to start at zero, as shown in Figure 16.

DOI: 10.3217/978-3-99161-057-1-109

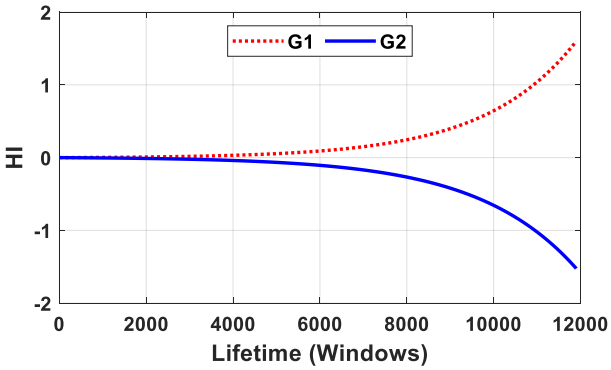

Figure 16 Constructed HI using generated data

As shown in Figure 16, the Health Indicator (HI) for G1 exhibits an increasing trend, while for G2, it shows a decreasing trend. This suggests that the HI can be used for health monitoring, even with real data. Although a specific threshold cannot be defined, an adaptive threshold could be a potential solution, requiring further investigation.

6 CONCLUSIONS

This study presents a framework to compress, reduce, and fuse raw data collected from a sensor network into a HI for monitoring road infrastructure using FBG sensor network that produces a sheer volume of data. The integration of sensor data processing, feature extraction, and machine learning methods enables the detection of damage in infrastructure, ensuring timely maintenance interventions. Key findings of this study are as follows:

- Based on experimental tests, it has been confirmed that the sensor response is dependent on its distance from the damage.
- The monotonicity metric is effective in identifying features sensitive to damage propagation and refining features before fusion.
- The use of the first principal component as a health indicator demonstrates its effectiveness in tracking damage progression. In experimental tests, the health indicator's trend helped identify damage once it exceeded a threshold, though further validation is needed to establish a universal failure threshold for real-world applications.
- The proposed HI meets the key criteria for an optimal HI, including detectability and separability, making it acceptable based 2VP. Additionally, trendability can be achieved by taking the absolute value of the HI if needed.
- The constructed HI can be used for RUL estimation using a prognosis model, provided the threshold is known. However, determining a reliable threshold remains a challenge for real-world applications.
- The proposed framework is sensor-independent, except for some specific pre-processing steps that vary for each sensor. This framework can be implemented for infrastructure monitoring using large-scale sensor networks for efficient SHM.

In conclusion, the methodology introduced in this study holds great promise for the future of infrastructure health monitoring. With further refinement and validation, it has the potential to make road maintenance more efficient and cost-effective.

ACKNOWLEDGMENTS

This study is funded by the Port of Antwerp-Bruges, project 48231 "Durable Pavements for Port area - Heavily loaded pavements: exploration and in-depth study". The research team also thanks Com&Sens for their technical support during installation and data collection.

REFERENCES

[1] Barbieri dm, Lou b. Instrumentation and testing for road condition monitoring–a state-of-the-art review. NDT & E International. 2024 Jun 12:103161.
[2] Bajwa R, Coleri E, Rajagopal R, Varaiya P, Flores C. Pavement performance assessment using a cost-effective wireless accelerometer system. Computer-Aided Civil and Infrastructure Engineering. 2020 Sep;35(9):1009-22.
[3] Memisoglu Apaydin N, Zulfikar AC, Cetindemir O. Structural health monitoring systems of long-span bridges in Turkey and lessons learned from experienced extreme events. Journal of Civil Structural Health Monitoring. 2022 Dec;12(6):1375-412.
[4] Kavitha S, Daniel RJ, Sumangala K. High performance MEMS accelerometers for concrete SHM applications and comparison with COTS accelerometers. Mechanical Systems and Signal Processing. 2016 Jan 1;66:410-24.
[5] Ghaderiaram A, Schlangen E, Fotouhi M. Structural Fatigue Life Monitoring with Piezoelectric-Based Sensors: Fundamentals, Current Advances, and Future Directions. Sensors. 2025 Jan 8;25(2):334.
[6] Saafi M, Sayyah T. Health monitoring of concrete structures strengthened with advanced composite materials using piezoelectric transducers. Composites Part B: Engineering. 2001 Jan 1;32(4):333-42.
[7] Alavi AH, Hasni H, Lajnef N, Chatti K. Continuous health monitoring of pavement systems using smart sensing technology. Construction and Building Materials. 2016 Jul 1;114:719-36.
[8] Michalcová L, Bělský P, Petrusová L. Composite panel structural health monitoring and failure analysis under compression using acoustic emission. Journal of Civil Structural Health Monitoring. 2018 Sep;8(4):607-15.
[9] Lovejoy SC. Acoustic emission testing of beams to simulate SHM of vintage reinforced concrete deck girder highway bridges. Structural Health Monitoring. 2008 Dec;7(4):329-46.
[10] Carboni M, Crivelli D. An acoustic emission based structural health monitoring approach to damage development in solid railway axles. International Journal of Fatigue. 2020 Oct 1;139:105753.
[11] Wang Y, Yao H, Wang J, Xin X. Distributed optical fiber sensing system for large infrastructure temperature monitoring. IEEE Internet of Things Journal. 2021 Jul 19;9(5):3333-45.
[12] Chen B, Zhu Z, Su Z, Yao W, Zheng S, Wang P. Optical fiber sensors in infrastructure monitoring: a comprehensive review. Intelligent Transportation Infrastructure. 2023;2:liad018.
[13] Velha P, Nannipieri T, Signorini A, Morosi M, Solazzi M, Barone F, Frisoli A, Ricciardi L, Eusepi R, Icardi M, Recchia G. Monitoring large railways infrastructures using hybrid optical fibers sensor systems. IEEE Transactions on Intelligent Transportation Systems. 2019 Nov 7;21(12):5177-88.
[14] Chan TH, Yu L, Tam HY, Ni YQ, Liu SY, Chung WH, Cheng LK. Fiber Bragg grating sensors for structural health monitoring of Tsing Ma bridge: Background and experimental observation. Engineering structures. 2006 Apr 1;28(5):648-59.
[15] Wang J, Han Y, Cao Z, Xu X, Zhang J, Xiao F. Applications of optical fiber sensor in pavement Engineering: A review. Construction and Building Materials. 2023 Oct 12;400:132713.
[16] Golmohammadi A, Hasheminejad N, Hernando D. An Innovative Data Analysis Approach via Peak-Counting–Based Segmentation for Pavement Monitoring Using FBG Sensors. Journal of Testing and Evaluation. 2025 Mar 1;53(2).
[17] Golmohammadi A, Hasheminejad N, Hernando D, Vanlanduit S. Performance assessment of discrete wavelet transform for de-noising of

DOI: 10.3217/978-3-99161-057-1-109

FBG sensors signals embedded in asphalt pavement. Optical Fiber Technology. 2024 Jan 1;82:103596.
[18] Santos AD, Silva MF, Sales CS, Fernandes CS, Sousa MJ, Costa JC, Souza RM. Software development for acquisition and data management in optical sensor networks. In2014 IEEE International Instrumentation and Measurement Technology Conference (I2MTC) Proceedings 2014 May 12 (pp. 96-101). IEEE.
[19] Wang T, Bhuiyan MZ, Wang G, Rahman MA, Wu J, Cao J. Big data reduction for a smart city's critical infrastructural health monitoring. IEEE Communications Magazine. 2018 Mar 15;56(3):128-33.
[20] Khoa NL, Zhang B, Wang Y, Chen F, Mustapha S. Robust dimensionality reduction and damage detection approaches in structural health monitoring. Structural Health Monitoring. 2014 Jul;13(4):406-17.
[21] Hassani S, Dackermann U, Mousavi M, Li J. A systematic review of data fusion techniques for optimized structural health monitoring. Information Fusion. 2024 Mar 1;103:102136.
[22] Wu RT, Jahanshahi MR. Data fusion approaches for structural health monitoring and system identification: Past, present, and future. Structural Health Monitoring. 2020 Mar;19(2):552-86.
[23] Moradi M, Broer A, Chiachío J, Benedictus R, Loutas TH, Zarouchas D. Intelligent health indicator construction for prognostics of composite structures utilizing a semi-supervised deep neural network and SHM data. Engineering Applications of Artificial Intelligence. 2023 Jan 1;117:105502.
[24] Coble J, Hines JW. Identifying optimal prognostic parameters from data: a genetic algorithms approach. InAnnual Conference of the PHM Society 2009 (Vol. 1, No. 1).
[25] Zhou H, Huang X, Wen G, Lei Z, Dong S, Zhang P, Chen X. Construction of health indicators for condition monitoring of rotating machinery: A review of the research. Expert Systems with Applications. 2022 Oct 1;203:117297.
[26] Golmohammadi A, Hernando D, Hasheminejad N. Advanced data-driven FBG sensor-based pavement monitoring system using multi-sensor data fusion and an unsupervised learning approach. Measurement. 2025 Jan 1;242:115821.
[27] Hernando D, Tavalaei SG, Hasheminejad N, Van Den Bergh W, Voet E. Exploring the use of fiber Bragg grating sensors for monitoring the structural response of asphalt pavements. InBituminous Mixtures and Pavements VIII 2024 Jun 21 (pp. 708-716). CRC Press.
[28] Saidi L, Ali JB, Bechhoefer E, Benbouzid M. Wind turbine high-speed shaft bearings health prognosis through a spectral Kurtosis-derived indices and SVR. Applied Acoustics. 2017 May 1;120:1-8.